

Accumulation of Metals by Bacteriogenic Iron Oxides in a Subterranean Environment

F. G. FERRIS

Department of Geology
University of Toronto
Toronto, Ontario, Canada

K. O. KONHAUSER

School of Earth Sciences
University of Leeds
Leeds, England

B. LYVÉN

Department of Analytical and Marine Chemistry
Chalmers University
Göteborg, Sweden

K. PEDERSEN

Department of Cell and Molecular Biology
Microbiology Section
University of Göteborg
Göteborg, Sweden

Bacteriogenic iron oxides (BIOS) and groundwater samples were collected from 66 to 432 m underground at the Äspö Hard Rock Laboratory near Oskarshamn, Sweden. The twisted, iron oxide-encrusted stalks of the lithoautotrophic ferrous iron-oxidizing bacterium Gallionella ferruginea were prominent in the BIOS samples. A wide variety of heterotrophic bacteria, including stalked forms resembling Caulobacter or Hyphomicrobium species, were also present. Energy dispersive x-ray spectroscopy, selected area electron diffraction, and x-ray diffraction analyses confirmed that the BIOS samples contained only poorly ordered (amorphous) hydrous ferric oxide. Inductively coupled plasma emission spectroscopy revealed iron oxide contents that varied from 60% to 90% (dry weight basis). Metal concentrations in filtered groundwater ranged from ~10 mM for Na to 10^{-4} mM or less for Co, Cu, Cr, and Zn. Intermediate concentrations were recorded for Fe and Mn ($\sim 10^{-2}$ mM). Solid-phase metal concentrations in the BIOS spanned the 10^{-2} to 10^{-5} mmol/kg range. Metal distribution coefficients (K_d values), calculated as the ratio between BIOS and dissolved metal concentrations, revealed solid-phase enrichments that, depending on the metal, extended from $\sim 10^0$ to nearly 10^5 . At the same time, however, a distinct trend of K_d values decreasing with increasing iron oxide content was evident for each metal, implying that metal uptake was strongly

Received 2 July 1998; accepted 1 December 1998.

This work was supported by the Natural Science and Engineering Research Council of Canada, the University of Leeds Academic Development Fund, The Swedish Institute, The Swedish Foundation for International Cooperation in Research and Higher Education, and the Swedish Nuclear Fuel and Waste Management Company. We also thank Vernon Phoenix for assistance with transmission electron microscopy.

Address correspondence to Dr. F. G. Ferris, Department of Geology, University of Toronto, 22 Russell St., Toronto, Ontario, Canada M5S 3B1. E-mail: ferris@quartz.geology.utoronto.c a

influenced by the relative proportion of bacterial organic matter in the composite solids. The metal accumulation properties of the BIOS suggest an important role for intermixed iron oxides and bacterial organic matter in the transport and fate of dissolved metals in groundwater systems.

Keywords bacteria, metals, iron oxides, subterranean

The behavior of bacteria as geochemically reactive solids can be inferred from extensive research documenting their performance as sorbents of dissolved metals and as nucleation templates for a wide range of authigenic minerals (Fortin et al. 1997; Konhauser 1998). This reactivity stems directly from the presence of amphoteric surface-functional groups (i.e., carboxyl, phosphoryl, and amino constituents) that are associated with structural polymers in the cell walls and external sheaths or capsules of individual cells (Beveridge et al. 1997). Direct interactions between these surface-functional groups and dissolved metals account for the sorptive properties of bacteria (Fein et al. 1997), whereas sorbed metals provide discrete sites for subsequent mineral nucleation and precipitation reactions (Warren and Ferris 1998).

Metals that are prone to hydrolysis in solution tend to sorb strongly and specifically to surfaces of reactive solids, including bacterial cells (Stumm and Morgan 1996; Warren and Ferris 1998). Ferric iron, in particular, is bound tenaciously by bacteria and commonly undergoes precipitation to form hydrous iron oxide coatings on cell surfaces (Ferris et al. 1989; Fortin et al. 1993; Konhauser 1997). These iron oxide precipitates are highly reactive themselves (Fuller et al. 1993; Waite et al. 1994; Anisworth et al. 1994) and effectively constitute a secondary sorbent phase for dissolved metals on the bacteria.

Because of their ubiquitous distribution and reactive surface properties, hydrous iron oxides are considered the dominant sorbents of dissolved metals in aquatic environments (Stumm and Morgan 1996). This perception is tempered, somewhat, by work showing that natural iron oxides often contain significant amounts of organic matter, including intact bacterial cells (Ferris et al. 1989; Filella et al. 1993; Fortin et al. 1993; Konhauser 1997, 1998). This intermixing of iron oxides and organic matter produces composite multiple-sorbent solids with highly variable metal retention properties (Warren and Zimmerman 1994a; Ingri and Widerlund 1994; Tessier et al. 1996).

Although considerable effort has gone into investigating the effects of humic compounds on metal accumulation by iron oxides (Day et al. 1994; Zachara et al. 1994; Payne et al. 1996), the impact of bacteria has been generally neglected. Apparently, one reason for this is that most of the organic materials in soils and surface waters are collectively described as humic substances (Stumm and Morgan 1996). Nevertheless, as outlined above, clear and convincing evidence shows that not only do natural iron oxides contain bacteria but also they form directly on bacterial surfaces in response to heterogeneous nucleation and precipitation reactions (Konhauser 1997; Warren and Ferris 1998). The present investigation was therefore undertaken to evaluate the extent to which dissolved metals partition into bacteriogenic iron oxides (BIOS) in a deep, hard rock, groundwater environment.

Methods

Sample Collection

BIOS were collected in the tunnel of the Äspö Hard Rock Laboratory (HRL) near Oskarshamn on the east coast of Sweden. Several major fracture zones that trend NE–SW in the area through the granitic bedrock intersect the 460-m-deep facility. Iron oxide precipitates

TABLE 1 Bulk composition of Äspö bacteriogenic iron oxides with respect to the total iron content of the precipitates

Sample	Depth (m)	mmol/kg Fe ^a	mg/g Fe(OH) ₃ ^b	Percent	
				Fe(OH) ₃ ^b	Residual organics ^c
1	432	7804	833	83.3	16.7
2A	296	7022	750	75.0	25.0
2B	296	6028	644	64.4	35.6
3	189	7001	748	74.8	25.2
4A	131	8405	898	89.8	10.2
4B	131	7720	824	82.4	17.6
5	66	6296	672	67.2	32.8

^aThe Fe concentration reported for sample 2B was determined by ICP-mass spectrometry (MS). The Fe content of all other samples was measured by ICP-AES. With both instruments the relative standard deviations for measurement of iron concentrations were less than $\pm 10\%$ of the reported values.

^bCalculated using a formula weight of 106.85 for hydrous ferric oxide, Fe(OH)₃.

^cCalculated based on the iron oxide content of the samples as 100 minus the percent Fe(OH)₃. Light microscopy, transmission electron microscopy, selected area electron diffraction, and bulk powder x-ray diffraction established that the samples did not contain any detrital rock fragments or other mineral debris. This indicated that the residual mass was composed of organic matter derived from *G. ferruginea* and other bacteria in the iron oxide precipitates.

develop commonly at locations where neutral to slightly alkaline (pH 7.0 to 8.0) ground-water enters the tunnel through hydraulically conductive fracture zones (Laaksoharju and Skårman 1995). Previous work at Äspö has established that the formation of these iron oxide precipitates is related principally to extensive oxidation of Fe(II) and growth of the stalk-forming bacterium *Gallionella ferruginea* (Pedersen and Karlson 1995; Pedersen 1997). For the present investigation, we collected samples from sites 66 to 432 m underground (Table 1).

The BIOS precipitates were recovered with sterile plastic spatulas and transferred directly into 200-mL polypropylene tubes. After the precipitates had settled by gravity to the bottom of the tubes (in ~ 5 min), excess water was decanted to accommodate additional sample collection. This procedure continued at each sampling site until ~ 30 mL of material was accumulated. The collected BIOS precipitates were a homogeneous orange-brown color and exhibited a loosely aggregated morphology. Water sample were collected at the same time, filtered through 0.22- μ m (pore-size) filters into 200-mL polypropylene tubes, and acidified to a final concentration of 5% (v/v) HCl. All sample tubes were sealed with screw caps and stored at 4°C in a refrigerator until chemical analyses.

Chemical and Mineralogical Analyses

The BIOS were concentrated on 0.45- μ m (pore-size) filters to remove excess water. The samples were then dried in an oven at 80°C and ground into a fine powder with an agate mortar and pestle. After dissolution in aqua regia, the samples were dried on a hot plate and redissolved in 5% (v/v) HCl. Total metal concentrations of the BIOS and water samples were measured with a Fisons ARL Maxim inductively coupled plasma atomic emission spectrometer (ICP-AES).

Hydroxylamine extraction was used to determine the solid-phase distribution of metals between the oxide and residual organic matter fraction in BIOS sample 2B from the 296-m

underground site (Table 1). The wet sample was resuspended in deionized distilled water at a concentration of 14 mg (dry wt) per milliliter. For measurement of the total metal concentration in the sample, 0.5 mL of the suspension was digested at 65°C for 24 h in 8.0 mL (final volume) of 32.5% (v/v) HNO₃. The BIOS were extracted from the digest with 0.043 M NH₂OH · HCl in 27% (v/v) acetic acid, followed by filtration through 0.22- μ m filters, to determine the concentration of metals associated directly with the oxide fraction of the samples (Landström and Tullborg 1995). Metal concentration were measured with a VG-PQ 1 ICP-MS. The difference between the total metal and the oxide metal concentrations provided an estimate of the metal content of the residual bacterial organic fraction in the BIOS.

Powder x-ray diffraction was used to evaluate the mineralogy and crystallinity of the BIOS precipitates. The samples were dried at 35°C and then analyzed with an INEL XRG 3000 diffractometer using a curved position-sensitive detector and Cu K α radiation (Institute for Energy Technology, Kjeller, Norway).

Microscopic Analyses

For light microscope, wet mounts of the BIOS were prepared under coverslips on glass slides. The specimens were then examined and photographed with an Olympus BH-2 photomicroscope equipped with differential interference contrast optics.

We used transmission electron microscopes (TEM) to inspect BIOS whole mounts and thin sections of specimens embedded in plastic resin. The whole mounts were prepared by floating Formvar-carbon-coated 200-mesh copper grids on small sample droplets for several minutes. Excess sample was then carefully removed by using filter paper, and the grids were allowed to air-dry.

To embed samples for thin-sectioning, specimens were fixed for 2 h with 2.0% (v/v) glutaraldehyde (final concentration in water from the sample site). The specimens were then dehydrated through use of a graded ethanol series and set in Agar 100 resin. After curing, thin sections were cut with a diamond knife on a Reichert–Jung ultramicrotome and mounted on Formvar-carbon-coated 200-mesh copper grids. The sections were then stained with uranyl acetate to enhance the electron contrast of the biological material. Specimens were examined with a Philips CM10 TEM operating at 100 kV, or with a Philips CM20 TEM equipped with a Link Analytical energy dispersive x-ray spectroscopy (EDS) system and are LZ-5 detector operating at 200 kV.

Results

Structure and Mineralogy

The distinct twisted stalks of the Fe(II)-oxidizing bacterium, *G. ferruginea*, were easily discerned by light microscopy in wet mounts of the BIOS (Figure 1). Coatings of fine-grained iron oxide precipitates were commonly seen on the *G. ferruginea* stalks and produced an elaborate highly porous solid-phase matrix. The presence of stalks with various degrees of iron oxide coatings introduced a further degree of structural heterogeneity, which can be attributed to ongoing microbial growth and mineral precipitation.

Although *G. ferruginea* was clearly prominent in the BIOS, different kinds of bacterial cells were visible within the precipitates. Lacking the unique and distinctive morphology of *G. ferruginea*, however, the other predominantly rod-shaped bacteria could not be identified by light microscopy. Instead microbiological studies have shown that a wide variety of heterotrophic bacteria are common in BIOS precipitates, growing by using organic matter produced in situ by chemoautotrophic *G. ferruginea* (Ghiorse 1984; Pedersen and Karlsson 1995; Pedersen 1997).

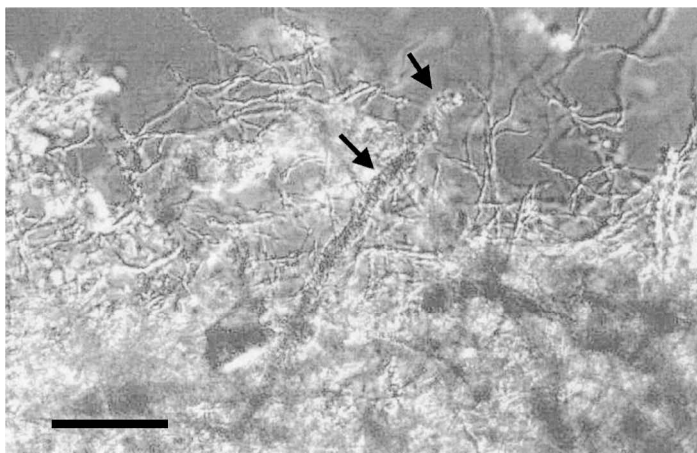


FIGURE 1 Differential interference contrast photomicrograph from a wet mount of a sample from the 296-m depth at Äspö, showing abundant twisted stalks produced by the Fe(II)-oxidizing bacterium, *G. ferruginea*. Coatings of fine-grained iron oxides of various thicknesses are clearly in evidence (arrows) on the stalks of *G. ferruginea* (bar = 20 μm).

In whole mounts and thin sections of BIOS specimens examined by TEM, iron oxide precipitates were visible not only as coatings on individual bacterial cells, including stalked bacteria resembling *Hyphomicrobium* or *Caulobacter* species (Figures 2A and 2B), but also as deposits within fibrous extracellular capsular material surrounding many of the bacteria (Figure 2C). The precipitates generated strong peaks for Fe by EDS (Figure 3) and typically exhibited a granular morphology that emerged from the aggregation of individual crystallites ~ 20 nm in diameter (Figure 2D). Electron diffraction of selected areas gave weak, diffuse patterns indicative of poorly ordered material with very little long-range crystalline structure. Similar results were obtained with bulk powder x-ray diffraction, which failed to yield any peaks indicative of crystalline material (e.g., rock fragments or other mineral debris).

As shown in Table 1, the BIOS were dominated compositionally by Fe, which, as hydrous ferric oxide, $\text{Fe}(\text{OH})_3$, accounted for 64% to 89% of the solid mass. The residual mass must be derived mostly from bacterial organic matter, in accordance with light microscopic and TEM observations as well as powder x-ray diffraction results.

Dissolved Metal Concentrations

The dissolved metal concentrations in the Äspö groundwater samples spanned the 10 to 10^{-5} mM range (Table 2). Sodium concentrations were the highest of the measured dissolved metals, followed by iron and manganese. Other metals, including Co, Cu, Cr, and Zn, were present at the extreme low end of the concentration range.

The variation in dissolved metal concentrations between sampling sites at the Äspö facility was fairly low, as Table 2 shows. Typically, the molar concentration of metals were within the same order of magnitude at all sample sites. Differences across the sampling sites ranged from little more than twofold in the case of Na, to a maximum fivefold difference between sites for the lowest and highest concentrations of dissolved Fe. The only consistent trend of note among the dissolved metals was a slight increase in Na concentrations with depth.

TABLE 2 Dissolved metal concentrations in Äspö groundwater samples

Site	Depth (m)	Concentration (mM)						
		Na	Cu	Cr	Fe	Mn	Co	Zn
1	432	81.86	0.00023	0.0004	0.018	0.008	0.00029	0.00006
2	296	64.59	0.00016	0.0003	0.011	0.017	0.00009	0.00031
3	189	52.71	0.00009	0.0003	0.018	0.016	0.00009	bd
4	131	63.68	0.00016	0.0004	0.036	0.012	0.00017	0.00008
5	66	40.84	0.00014	0.0003	0.008	0.010	0.00007	bd

bd, below detection limit. The relative standard deviations for measurement of individual metal concentrations were less than $\pm 10\%$ of the reported values.

Solid-Phase Metal Concentrations

The solid-phase metal concentrations of the BIOS are shown in Table 3. In addition to Fe (Table 1), Na and Mn exhibited the highest concentrations, exceeding 10 mmol/kg at all sites. Cobalt was generally around the 5.0 to 7.0 mmol/kg concentration range, whereas Zn, Cu, and Cr concentrations extended from near 0.02 mmol/kg to 0.3 mmol/kg. In comparison

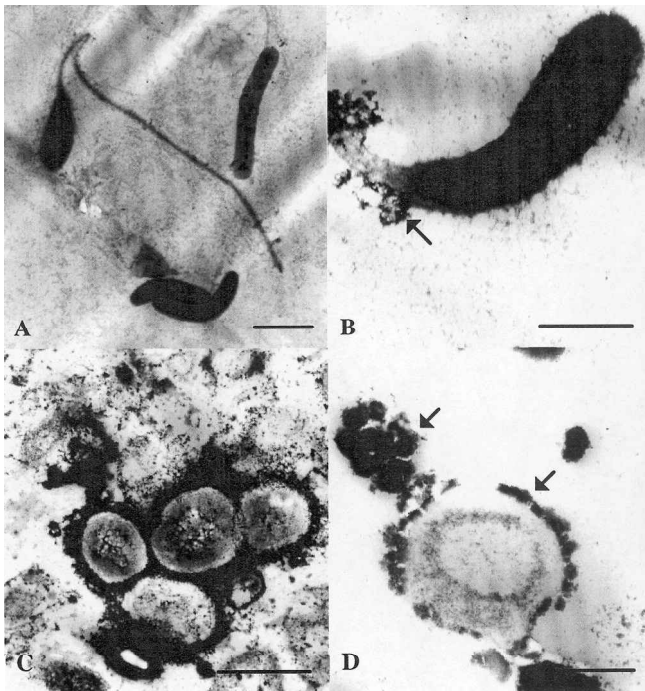


FIGURE 2 Transmission electron micrographs showing (A) a variety of bacterial cells, including a stalked bacteria (bar = 1.0 μm), and (B) cell-surface iron oxide precipitates (arrow) in a whole mount of BIOS sample 2A from 296 m underground (bar = 0.5 μm). (C) Accumulation of iron oxide precipitates around encapsulated bacteria in a thin section of BIOS sample 1 from 432 m underground, and (D) aggregation of fine-grained iron oxide precipitates on the surface of thin-sectioned bacterial cells in BIOS sample 4 from 131 m underground (bars = 0.5 μm).

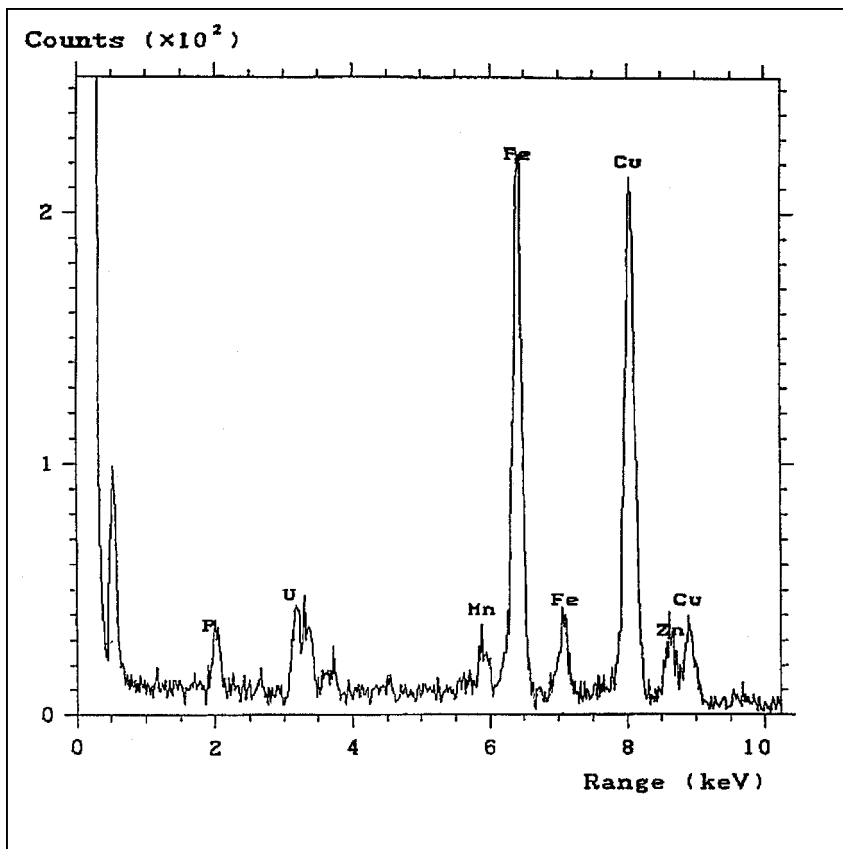


FIGURE 3 An energy dispersive x-ray spectrum from the iron oxide precipitates around the bacterial cell shown in Figure 2D. The Cu ($K\alpha$ and $K\beta$) peaks are from the support grid, and the U is from the stain used to enhance the electron contrast of the biological material; Fe ($K\alpha$ and $K\beta$), Mn, Zn, and P peaks are from the specimen.

with the water samples (Table 2), the metal concentrations in the BIOS were relatively high, implying that the dissolved metals had partitioned readily into the solid-phase precipitates.

Figure 4 shows for BIOS sample 2B the percentage of total solid-phase metal associated with the residual organic fraction, plotted against the percentage associated with the oxide fraction. Nearly 50% to 100% of the metals concentrated in the BIOS were retained by the oxide fraction. Of the five metals analyzed in the single extracted sample, Zn, Co, and Cu exhibited a moderate degree of affinity for the residual fraction at ~20%, 25%, and 50% of their total solid-phase concentrations, respectively. Conversely, Na and Mn were associated principally with the oxide fraction of the samples.

Relationships Between Dissolved and BIOS Metal Concentrations

Trace metal distribution coefficients (K_d values) were calculated in accordance with the conventional operational definition as the ratio between solid and dissolved metal concentrations [Me_{BIOS}] and [$Me_{\text{Dissolved}}$], respectively (Stumm and Morgan 1996):

$$K_d = [Me_{\text{BIOS}}] / [Me_{\text{Dissolved}}]$$

TABLE 3 Bulk solid-phase metal concentrations in the Äspö bacteriogenic iron oxides

Sample	mmol					
	Na	Cu	Cr	Mn	Co	Zn
1	57.85	0.03	0.19	18.57	6.41	0.032
2A	52.76	0.02	0.30	91.41	5.44	0.076
2B	100.39	0.13	nd	66.30	6.45	0.380
3	47.84	0.02	0.31	95.70	5.36	0.015
4A	34.32	0.03	0.25	20.45	6.10	0.018
4B	36.92	0.04	0.26	22.07	6.78	0.030
5	66.15	0.05	0.38	78.41	5.37	0.076

nd, not determined. Concentrations reported for sample 2B were determined by ICP-MS. The metal contents of all other samples were measured by ICP-AES. With both instruments the relative standard deviations for measurement of individual metal concentrations were less than $\pm 10\%$ of the reported values.

The highest K_d values (nearly 10^5) were computed for Co partitioning into the BIOS, whereas Na yielded low K_d values, near 1.0 (Figure 5). Intermediate K_d values, 10^2 to $> 10^3$, were obtained with Cr, Cu, Mn, and Zn.

Between-sample differences in K_d values for an individual metal were small, typically on the order of two- to threefold, particularly in comparison with the order of magnitude variations evident between the K_d values of different metals; however, a distinct trend of decreasing K_d with increasing iron oxide content was noted for each metal (Figure 5). This implies that the accumulation of metals by BIOS depends on the relative proportion of microbial biomass and iron oxide in the composite solid phase.

Discussion

In groundwater systems, marked redox and oxygen gradients commonly develop as meteoric or surface waters recharge the subterranean environment. Such gradients provide ideal

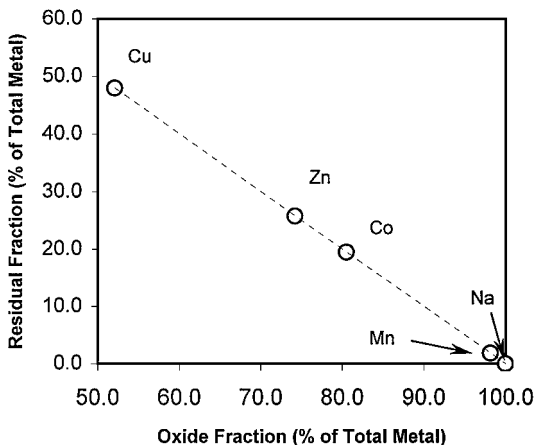


FIGURE 4 Relative distribution of metals in the oxide and residual fractions of Äspö sample 2B from the 296-m depth, expressed as a percentage of the total solid-phase concentration of metal.

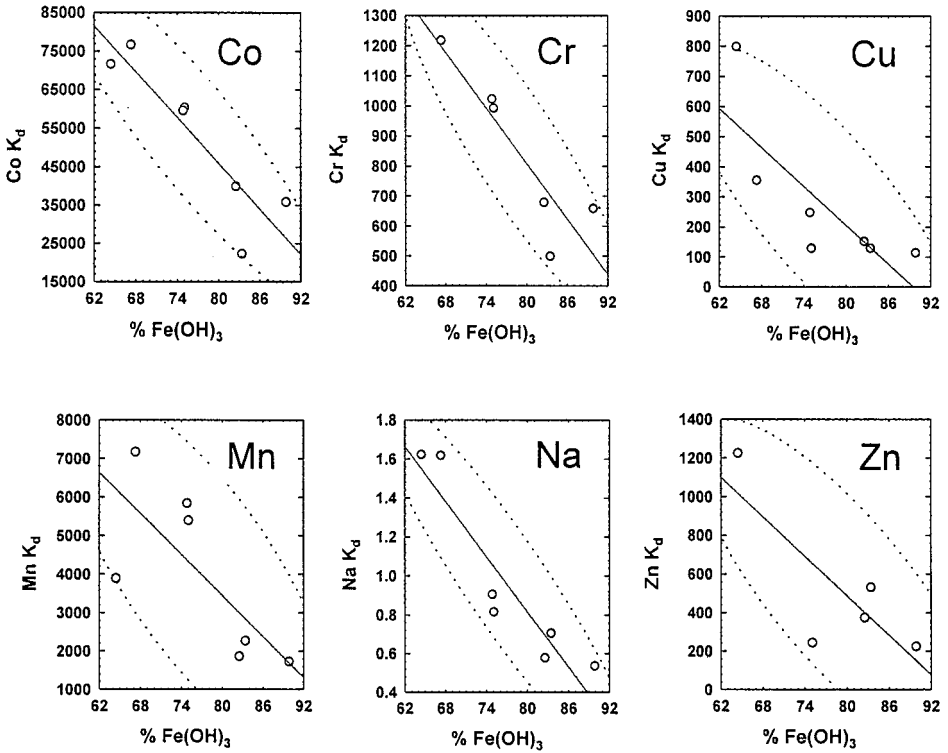


FIGURE 5 Metal distribution coefficients (K_d values, L/kg) as a function of the weight percent $\text{Fe}(\text{OH})_3$ in the bacteriogenic iron oxides. Dashed lines correspond to 90% elliptical confidence intervals for bivariate normal probability distributions of values around a decreasing trend (solid line) in K_d with respect to weigh percent $\text{Fe}(\text{OH})_3$ in the bacteriogenic iron oxides (STATISTICA v. 5.0).

habitats for many different bacteria, including lithoautotrophic and heterotrophic species (Pedersen 1997). Among the lithoautotrophs are iron oxidizers such as *G. ferruginea*, which generate chemical energy for metabolic processes through the oxidation of reduced ferrous iron. The energy gained by this lithoautotroph is used to reduce dissolved inorganic carbon to organic matter (Hallbeck and Pedersen 1991, 1995) and generates oxidized ferric iron, which is highly prone to precipitation as hydrous iron oxides (Stumm and Morgan 1996). The organic matter produced by lithoautotrophs such as *G. ferruginea*, in turn, supports the growth of heterotrophic bacteria (Pedersen 1997).

The formation of iron oxide precipitates on the stalks of *G. ferruginea* is a well-documented phenomenon interpreted as a direct consequence of metabolic ferrous iron oxidation (Hallbeck and Pedersen 1995). Similarly, accumulation of iron oxide in association with heterotrophic bacteria has been reported in environments in which high concentrations of ferric iron are produced by either chemical or bacterial oxidation of ferrous iron (Ferris et al. 1989; Fortin et al. 1993; Konhauser and Ferris 1996; Konhauser 1997, 1998). In all of these cases, and at Äspö, the accretion of BIOS can be explained by a continuum of surface complexation–nucleation–precipitation reactions (Warren and Ferris 1998).

The progression of iron oxide precipitation on the surface of bacteria depends critically on the total supply of dissolved ferric iron and availability of reactive amphoteric sorption sites (i.e., carboxyl or phosphoryl groups) on individual cells (Beveridge et al. 1997; Fein et al. 1997; Konhauser 1997). When the amount of ferric iron subject to precipitation is high

in comparison with the sorption capacity of the bacteria, the resulting solid phase will be dominated by iron oxide (Warren and Ferris 1998). Similarly, decreased amounts of ferric iron or increased microbial biomass will produce BIOS that contain a lower proportion of iron oxide. These relationships can account for the variations in iron oxide content of BIOS from the Äspö tunnel.

The chemical composition of groundwater at the Äspö Hard Rock Laboratory (HRL) is modulated by mixing of fresh meteoric water, modern Baltic Sea water, old glacial meltwater, and deep saline groundwaters (Laaksoharju and Skårman 1995). Because of this, shallow waters tend to be somewhat fresher and have lower Na concentrations than does the deeper groundwater. At the same time, the predominance of granitic bedrock at all levels of the HRL donates only very small amounts of dissolved metals to the groundwater through chemical weathering processes (Landström and Tullborg 1995; Stumm and Morgan 1996). In these respects, the measured dissolved metal concentrations conform well with the documented hydrogeochemical and geological characteristics of the Äspö facility.

The iron oxide content and trace metal concentrations of the BIOS samples agree favorably with measurements on rock fracture-filling mineral precipitates collected at Äspö (Landström and Tullborg 1995). Similarly, the relative magnitude of calculated K_d values generally parallels those obtained for various metals and iron oxide-rich particulates in a wide range of aquatic environments (Ingri and Widerlund 1994; Warren and Zimmerman 1994a). There is a broad consensus, however, that the solid-phase partitioning of dissolved metals and the associated K_d values are quite sensitive to the composition of heterogeneous solid materials (Warren and Zimmerman 1994b; Radovanovic and Koelmans 1998). Specifically, the incorporation of organic matter into particulate sorbent phases can dramatically affect metal partitioning and can support large increases in K_d values (Zachara *et al.* 1994; Payne *et al.* 1996).

One of the major effects of organic incorporation into iron oxides is a lowering of the isoelectric point of the composite solid (Day *et al.* 1994). At constant pH, this tends to promote increased solid-phase partitioning of trace metals, as is observed with increasing bacterial organic matter in the BIOS precipitates (Zachara *et al.* 1994; Tessier *et al.* 1996; Payne *et al.* 1996). Enhanced uptake of dissolved metals by organic-rich BIOS corresponds additionally to a higher surface density of reactive sorption sites on bacterial cells in comparison with that on iron oxides (Fein *et al.* 1997; Warren and Ferris 1998).

Additional factors that can influence K_d values of heterogeneous solids such as BIOS include differences in affinity of metal sorption between constituent organic and inorganic sorbents as well as the aging of fresh mineral precipitates. Some metals, notably Cu and to a lesser extent Zn, commonly exhibit a high affinity for the organic fraction of suspended particulates in aquatic systems (Warren and Zimmerman 1994a). This behavior was clearly evident with the BIOS sample that was subjected to hydroxylamine extraction. At the same time, aging of freshly precipitated hydrous iron oxides in water can lead to a release of some sorbed metals, whereas others (e.g., Co) are retained and incorporated into the oxide during crystal growth (Fuller *et al.* 1993; Anisworth *et al.* 1994). Enhanced retention of Co in response to iron oxide aging is consistent with the high K_d values for this metal in the BIOS samples.

In computational studies of metal dispersion in groundwater systems, the influence of solid-phase reactivity and hydraulic conductivity, while substantial, seems to be less critical than the abundance and distribution of reactive solids, such as iron oxide banding in unconsolidated sand bodies (Thompson *et al.* 1996). These findings attach a high degree of importance to multicomponent interactions likely to exercise control over both the extent and spatial pattern of solid-phase metal partitioning. On each account, the accretion of BIOS figures prominently, in that cell-surface precipitation reactions serve to localize iron oxide deposition in places where bacteria are growing, and bacterial cell-derived organic

matter enhances solid-phase metal accumulation. The complex interplay between bacterial and geochemical processes seems to be emerging as a new focal point for environmental chemistry (Warren and Ferris 1998), particularly as predictive modeling seeks increasingly to accommodate the physical, chemical, and biological heterogeneity of natural systems in a realistic manner (Thompson et al. 1996)

References

- Anisworth CC, Pilon JL, Gassman PL, Vandersluys WG. 1994. Cobalt, cadmium, and lead sorption to hydrous iron-oxide—residence time effect. *Soil Sci Soc Am J* 58:1615–1623.
- Beveridge TJ, Hughes MN, Lee H, Leung KT, Poole PK, Savvaidis I, Silver S, Trevors JT. 1997. Metal–microbe interactions: contemporary approaches. *Adv Microb Physiol* 38:177–243.
- Day GM, Hart BT, McKelvie ID, Beckett R. 1994. Adsorption of natural organic-matter onto goethite. *Colloids Surfaces A Physicochem Eng Aspects* 89:1–13.
- Fein JB, Daughney CJ, Yee N, Davis TA. 1997. A chemical equilibrium model for metal sorption onto bacterial surfaces. *Geochim Cosmochim Acta* 61:3319–3328.
- Ferris FG, Tazaki K, Fyfe WS. 1989. Iron oxides in acid mine drainage environments and their association with bacteria. *Chem Geol* 74:321–330.
- Filella M, Buffle J, Leppard GG. 1993. Characterization of submicrometer colloids in fresh-waters—evidence for their bridging by organic structures. *Water Sci Technol* 27:91–102.
- Fortin D, Leppard GC, Tessier A. 1993. Characteristics of lacustrine diagenetic iron oxyhydroxides. *Geochim Cosmochim Acta* 57:4391–4404.
- Fortin D, Ferris FG, Beveridge TJ. 1997. Surface-mediated mineral development by bacteria. *Rev Mineral* 35:161–180.
- Fuller CC, Davis JA, Waychunas GA. 1993. Surface chemistry of ferrihydrite. 2. Kinetics of arsenate adsorption and coprecipitation. *Geochim Cosmochim Acta* 57:2271–2282.
- Ghiorse WC. 1984. Biology of iron- and manganese-depositing bacteria. *Ann Rev Microbiol* 38:515–550.
- Hallbeck L, Pedersen K. 1991. Autotrophic and mixotrophic growth of *Gallionella ferruginea*. *J Gen Microbiol* 138:2657–2661.
- Hallbeck L, Pedersen K. 1995. Biofilm development by the stalk-forming and iron-oxidizing bacterium *Gallionella ferruginea* and evaluation of the benefits associated with the stalk. *Microb Ecol* 30:257–269.
- Ingri J, Widerlund A. 1994. Uptake of alkali and alkaline-earth elements on suspended iron and manganese in the Kalix River, Northern Sweden. *Geochim Cosmochim Acta* 58:5433–5442.
- Konhauser KO. 1997. Bacterial iron biomineralization in nature. *FEMS Microbiol Rev* 20:315–326.
- Konhauser KO. 1998. Diversity of bacterial iron mineralization. *Earth Sci Rev* 43:91–121.
- Konhauser KO, Ferris FG. 1996. Diversity of iron and silica precipitation by microbial mats in hydrothermal waters, Iceland. Implications for Precambrian iron formations. *Geology* 24:323–326.
- Laaksoharju M, Skärman C. 1995. Groundwater sampling and chemical characterization of the Äspö HRL tunnel in Sweden. SKB Äspölaboratoriet Progress Report 25-95-29. Stockholm, Sweden: Svensk Kärnbränslehantering AB, 131 pp.
- Landström O, Tullborg E-L. 1995. Interactions of trace elements with fracture filling minerals from the Äspö Hard Rock Laboratory. SKB Technical Report 95-13. Stockholm, Sweden: Svensk Kärnbränslehantering AB, 71 pp.
- Payne TE, Davis JA, Waite TD. 1996. Uranium adsorption on ferrihydrite—effects of phosphate and humic acid. *Radiochim Acta* 74:239–243.
- Pedersen K. 1997. Microbial life in deep granitic rock. *FEMS Microbiol Rev* 20:399–414.
- Pedersen K, Karlsson F. 1995. Investigations of subterranean microorganisms. SKB Technical Report 95-10. Stockholm, Sweden: Svensk Kärnbränslehantering AB, 222 pp.
- Radovanovic H, Koelmans AA. 1998. Prediction of in situ trace metal distribution coefficients for suspended solids in natural waters. *Environ Sci Technol* 32:753–759.

- Stumm W, Morgan JJ. 1996. Aquatic chemistry, 3rd ed. New York: John Wiley.
- Tessier A, Fortin D, Belzile N, DeVitre RR, Leppard GG. 1996. Metal sorption to diagenetic iron and manganese oxyhydroxides and associated organic matter: narrowing the gap between field and laboratory measurements. *Geochim Cosmochim Acta* 60:387–404.
- Thompson AFG, Schafer AL, Smith RW. 1996. Impacts of physical and chemical heterogeneity on cocontaminant transport in a sandy porous medium. *Water Resour Res* 32:801–818.
- Waite TD, Davis JA, Payne TE, Waychunas GA, Xu N. 1994. Uranium(VI) adsorption to ferrihydrite—application of a surface complexation model. *Geochim Cosmochim Acta* 58:5465–7037.
- Warren LA, Ferris FG. 1998. Continuum between sorption and precipitation of Fe(III) on microbial surfaces. *Environ Sci Technol* 32:2331–2337.
- Warren LA, Zimmerman AP. 1994a. The influence of temperature and NaCl on cadmium, copper, and zinc partitioning among suspended particulate and dissolved phases in an urban river. *Water Res* 28:1921–1931.
- Warren LA, Zimmerman AP. 1994b. The importance of surface-area in metal sorption by oxides and organic-matter in a heterogenous natural sediment. *Appl Geochem* 9:245–254.
- Zachara JM, Resch CT, Smith SC. 1994. Influence of humic substances on Co^{2+} sorption by a surface mineral separate and its mineralogical components. *Geochim Cosmochim Acta* 58:553–566.